Threshold t-channel factorization model and its application to $\gamma\gamma$ reactions

G. Alexander and U. Maor
School of Physics and Astronomy, Tel-Aviv University, Tel-Aviv 69978, Israel
(Received 1 July 1991)

The t-channel factorization model for a threshold integrated cross section is reviewed. Its applicability to $\gamma\gamma$ reactions is examined. It is argued that the model reproduces the enhancement observed in the diffractive channels of $\gamma\gamma \to 2$ neutral vector mesons and reproduces the total $\gamma\gamma$ cross section. The model's predictive power and limitations are discussed and it is utilized to reproduce the threshold enhancement observed in $\sigma(K^+p \to K^0\Delta^{++})$ at low energy.

PACS number(s): 13.65.+i, 12.40.−y, 13.60.−r, 13.75.−n

I. INTRODUCTION

A renewed interest in the mechanism of integrated cross sections near their threshold was triggered some time ago by the TASSO observation [1] of a large low-mass $\rho^0\rho^0$ enhancement in the two quasireal (no-tag) photon reaction $\gamma\gamma \to \rho^0\rho^0$. This first observation, which was subsequently supported by other experiments [2–5], shows the $\rho^0\rho^0$ enhancement to extend well below the nominal $\rho\rho$ threshold. The interpretation of this phenomenon in terms of a conventional $q\bar{q}$ resonance state is ruled out since the related $\gamma\gamma \to \rho^+\rho^-$ is too small to be accounted for by a pure isospin state [6,7]. The study of the $\rho\rho$ system was followed by many experiments covering the $\gamma\gamma \to V_1V_2$ channels [1–7] with light u, d, and s quarks. These experiments have revealed a very rich structure at low energies of the V_1V_2 final states. Such a diversity seems to be too rich to be described by a single mechanism. Inasmuch as some formation of $4q$ exotic states [8,9] may contribute to these reactions, there is neither an experimental nor a theoretical reason to assume the exclusiveness of the formation of $4q$ states in low energy $\gamma\gamma$ reactions [10].

Some experimental support for the identification of the $\rho^0\rho^0$ threshold peak as a predominantly (exotic) $J^P=2^+$ state has been reported. This claim, however, is not supported by a subsequent analysis of the $\gamma\gamma \to \rho^+\rho^-$ reaction [11]. Independent of this open question, which is addressed to in Sec. III, it is rather obvious that any detailed analysis of the $\gamma\gamma \to V_1V_2$ data at low energies requires a realistic estimate of a nonresonating background which may well be responsible for the bulk of the observed events. However, as is well known, the low-energy behavior of a multichannel reaction such as $\gamma\gamma \to V_1V_2$ is not well understood and is bound to be very complicated. The t-channel factorization model (TCFM) was suggested by us some years ago [12] as a simplified approach to this problem. The model estimates the low-energy $\gamma\gamma \to V_1V_2$ data by extrapolating from the high-energy regime where a factorization approach is well established [13]. How such an extrapolation should be formulated is, unfortunately, a matter of taste and an educated guess. The justification of such an *ad hoc* model depends, thus, on its capability to describe most, if not all, of the diffractive low-energy $\gamma\gamma$ reactions both on and off the photon mass shell. This being the case, we conclude that the ratio of the suggested exotic-state signals over the estimated background in the $\gamma\gamma \to V_1V_2$ is probably small. Fur- thermore, if such signals do exist, their experimental verification will be hard to prove.

The structure of our paper is as follows. In Sec. II we define the model and discuss our motivation in its construction. Section III is devoted to an overall display of our results for various $\gamma\gamma \to V_1V_2$ channels. Our estimates for quasireal $\gamma\gamma$ total cross section are given in Sec. IV and for tagged off-mass-shell photons in Sec. V. In Sec. VI we critically assess this model. To demonstrate the ability of the model to reproduce nonresonance threshold enhancements, we discuss in the same section, as an example, the reaction $K^+p \to K^0\Delta^{++}$. Finally, our conclusions are summarized in Sec. VII.

II. MODEL

The TCFM estimates low-energy integrated cross sections assuming the factorization of t-channel amplitudes with definite quantum numbers. We recall that factorization is a well-established property of scattering amplitudes in the high-energy limit [13]. For the reaction $a+b \to c+d$, we write

$$\frac{d\sigma}{dt} = \frac{1}{16\pi\lambda^2(s,m_a^2,m_b^2)} |f(s,t)|^2 , \tag{1}$$

where the flux factor (which we shall denote [12] also as F_{ab}) is

$$\begin{aligned} F_{ab} &= \lambda^2(s,m_a^2,m_b^2) \\ &= s^2 - 2s(m_a^2+m_b^2) + (m_a^2-m_b^2)^2 . \end{aligned} \tag{2}$$

Factorization of the spin average scattering amplitudes implies that

$$f_{ab\to cd} = \frac{f_{ay\to cy} f_{xb\to xd}}{f_{xy\to xy}} . \tag{3}$$

The factorization of the scattering amplitudes translates into three simple high-energy cross-section factorization relations.

(1) Through the optical theorem one obtains a factorization of the total cross section. Hence we expect that, in the high-energy limit,

$$\sigma_{\rm tot}^2(\pi p)=\sigma_{\rm tot}(\pi\pi)\sigma_{\rm tot}(pp) \ .$$

(2) In the high-energy limit, $F_{ab}=s^2$ and we obtain the factorization of the differential cross section $d\sigma/dt$.

(3) The integrated cross section for the reaction $a+b\to c+d$ is given by

$$\sigma(a+b\to c+d)=\int_{t_{\rm min}}^{t_{\rm max}}\frac{d\sigma}{dt} \ . \tag{4}$$

In the high-energy limit, $t_{\rm min}\to 0$ and $t_{\rm max}\to\infty$; accordingly, the factorization of $d\sigma/dt$ implies also the factorization of the integrated cross section $\sigma(a+b\to c+d)$.

Our basic dual assumption is that these factorization relations, and in particular the factorization of the integrated cross section, can be extrapolated to low energies. We suggest that such an extrapolation may serve as a reasonable average estimate of the low-energy background of the reaction $a+b\to c+d$. Evidently, this extrapolation must accommodate for the fact that at low energies the flux and phase-space factors, which were conveniently ignored in the high-energy limit, are strongly dependent on the external masses of the reactions. Thus we note that in the extreme low-energy region the threshold of the four reactions, related through Eq. (3), may be significantly different. In our approach we compensate explicitly for the different flux factors and account for the phase-space differences by applying factorization at a fixed outgoing center-of-mass momentum $p_{\rm out}^*$. In this way the phase-space factor $p_{\rm out}^*/W_{ij}$ (where W_{ij} is the $i+j$ rest mass) is approximately factorizable all the way down to threshold. Thus we get [12]

$$\sigma(a+b\to c+d)=\sum_i\frac{\sigma^i(a+y\to c+y)\sigma^i(x+b\to x+d)}{\sigma^i(x+y\to x+y)}\frac{F_{ay}F_{xb}}{F_{ab}F_{xy}} \ , \tag{5}$$

where the summation is over the various t-channel sets of quantum number contributing to the reaction $a+b\to c+d$. Furthermore, all the terms in Eq. (5) are evaluated at the same $p_{\rm out}^*$ value. Appropriately, we note that a reversed extrapolation back to the high-energy limit reduces Eq. (5) to the conventional factorization relation. We recall that any t-channel one-particle-exchange contribution to $\sigma(a+b\to c+d)$ vanishes at the threshold because of its diminishing phase-space factor. This is not necessarily the case for Eq. (5), which is supposed to account for more complicated processes in all channels.

When one of the produced final states is a wide resonance, as is the case in some of the $\gamma\gamma\to V_1V_2$ channels, we have to unfold the Breit-Wigner integration of the input cross section and then fold it back for the output cross section. Specifically, we write

$$\sigma(a+b\to R+d)=\int\tilde{\sigma}(a+b\to m+d)|I_{\rm BW}(m)|^2dm^2 \ , \tag{6}$$

where

$$I_{\rm BW}(m)=\frac{\sqrt{m_R\Gamma_R m/p^*}}{\pi(m_R^2-m^2-im_R\Gamma_R)} \quad \text{and} \quad \Gamma_R=\Gamma_0\left[\frac{p^*}{p_0^*}\right]^{2J+1}\frac{2(p_0^*)^2}{(p_0^*)^2+(p^*)^2} \ . \tag{7}$$

p^* and p_0^* are the (two) decay product momenta in the m and R rest frames, respectively. It is the unfolded cross section $\tilde{\sigma}(\gamma p\to mp)$ which is related to Eq. (5), and so we get

$$\sigma(\gamma\gamma\to V_1V_2)=\sum_i\int dm_1^2\int dm_2^2\frac{\tilde{\sigma}(\gamma p\to m_1p)\tilde{\sigma}(\gamma p\to m_2p)}{\sigma(pp\to pp)}\frac{F_{\gamma p}F_{\gamma p}}{F_{\gamma\gamma}F_{pp}}|I_{\rm BW}(m_1)|^2|I_{\rm BW}(m_2)|^2 \ . \tag{8}$$

The Breit-Wigner form we use [14], i.e., Eq. (7), factors out explicitly [1] the term m/p^* corresponding to a two-body decay mode. It is, as such, appropriate for our practical purposes. Since in our calculations we unfold and then fold back, we find that the final results are insensitive to this m/p^* term.

III. ESTIMATES FOR $\gamma\gamma\to V_1V_2$

In this section we shall present our detailed estimates for various $\gamma\gamma\to V_1V_2$ channels. Following Eq. (8), such calculations depend on the details of our kinematical factor and the cross-section input, i.e., the experimental integrated cross section for vector-meson photoproduction and elastic baryon-baryon scattering.

Our estimates for $\sigma(\gamma\gamma\to\rho^0\rho^0)$ are compared in Fig. 1 with the relevant data [1–5]. As can be seen, the TCFM describes the data well. In particular, the threshold enhancement extending below the nominal $\rho^0\rho^0$ threshold is reproduced. Implicit to our calculations is the assumption that $\gamma\gamma\to\rho^0\rho^0$ is diffractive all the way down to threshold. This assumption is well supported by the analysis [15,16] of the $\rho^0\to\pi^+\pi^-$ decay density matrix in the photoproduction $\gamma p\to\rho^0 p$ reaction. Following Eq. (8), we can trace the elements contributing to the final result.

(1) The kinematical factor $F_{\gamma p}^2/(F_{\gamma\gamma}F_{pp})$ diverges as $(1/P_{\rm out}^*)^2$. This was the main factor contributing to the threshold singularity obtained in a zero-width calculation [12]. This singularity is smoothed over by the folding

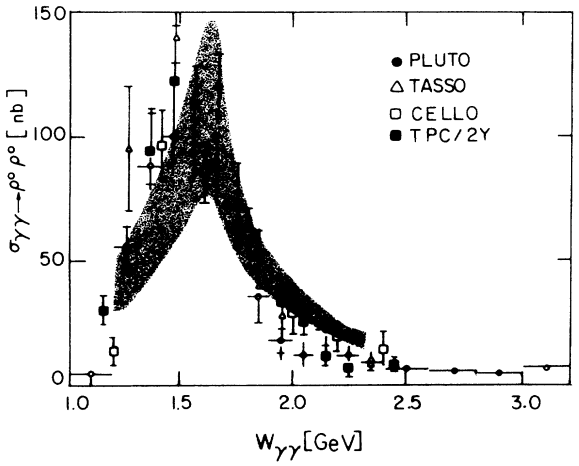

FIG. 1. Data compilation of $\sigma(\gamma\gamma\to\rho^0\rho^0)$ as a function of $W_{\gamma\gamma}$ compared with the expectation of the TCFM (shaded band).

procedure of Eq. (8).

(2) For the photoproduction $\gamma p\to\rho^0 p$, we have averaged over the CEA and ABBHHM data points [15,16] (see Fig. 2). For the purpose of unfolding the ρ width, using Eq. (6), one needs some algebraic representation for $\tilde{\sigma}(\gamma p\to mp)$ with fitted coefficients. We find it convenient to use a physically motivated four parameter expression

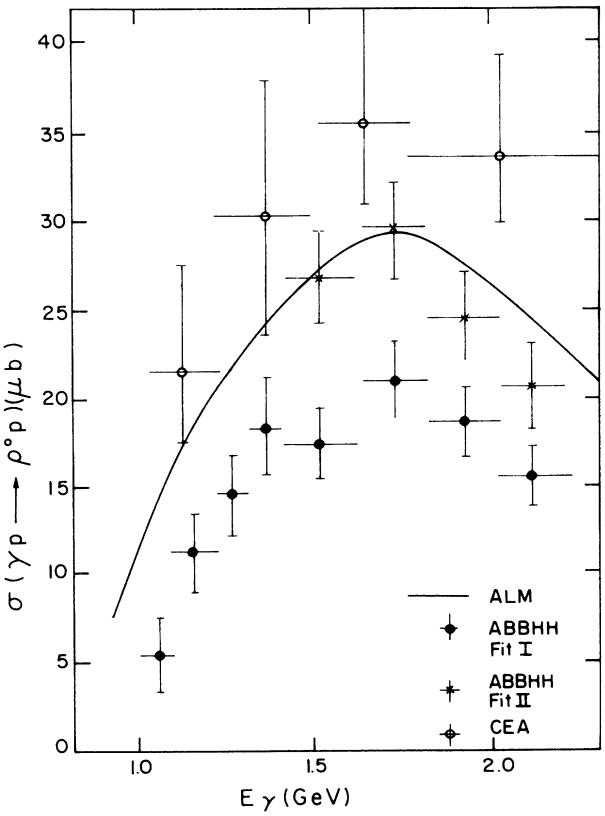

FIG. 2. Data compilation of low-energy $\sigma(\gamma p\to\rho^0 p)$ as a function of $W_{\gamma p}$. The solid line represents the input data taken from the present work and Ref. [12].

$$\tilde{\sigma}(\gamma p\to mp)=\left[\frac{p^*_{\rm out}}{W_{\gamma p}}\right]^{\alpha}\left[A+\frac{B}{W_{\gamma p}}+\frac{C}{W^2_{\gamma p}}\right]. \quad (9)$$

With this parametrization the approach to the threshold zero depends on the fitted parameter α, which turns out to be smaller than unity.

The result of our fit is that our input contains subthreshold cross sections. Unfortunately, there is a systematic difference between the CEA and ABBHHM data sets with the CEA data being consistently higher. We have thus checked the stability of our results. A simple polynomial fit produced very similar results with a falloff to threshold which is steeper than linear. We have further examined the case where only one of the CEA or ABBHHM input data sets is used in the analysis. We find that both data sets produce output results which are within our band. The output from the CEA data is close to the upper bound of our band, whereas the use of the ABBHHM data result in an output nearer to the lower bound.

We have constructed the input for the elastic pp scattering using a numerical interpolation through the experimental data points [17]. We note that below the pp inelastic threshold the elastic cross section has a minimum $\sigma^{\rm el}_{pp}\simeq 23$ mb at $p^*\simeq 0.35$ GeV. This is followed by a rapid rise as the energy decreases toward the pp threshold. This rise, which is attributed to the one-pion-exchange (OPE) mechanism, has been the subject of many partial-wave and phase-shift analyses [18]. For the TCFM application to $\gamma\gamma\to\rho^0\rho^0$, we need only the diffractive component of the pp elastic scattering close to threshold [19]. We note, however, that our output is not very sensitive to this part of the input. In fact, had we assumed a constant cross section say of $\sigma^{\rm el}_{pp}=23$ mb all the way down to threshold, we would have obtained a somewhat faster falloff of $\sigma(\gamma\gamma\to\rho^0\rho^0)$ below $W_{\gamma\gamma}=1.5$ GeV. Similar conclusions are inferred also from other calculations [19].

A critical dynamical facet of $\gamma\gamma\to\rho^0\rho^0$ may be obtained from the s-channel partial-wave analysis of this reaction. Unfortunately, however, the relevant experimental results are not conclusive. The TASSO experiment [1] obtains a significant $J^P=0^+$ component for $W_{\gamma\gamma}<1.6$ GeV and a sizable 2^+ contribution just above it. The decomposed partial waves do not show a resonance shape. The PLUTO Collaboration [5] finds a mixture of 0^+ and 2^+ for $1.2<W_{\gamma\gamma}<1.8$ GeV, but also reports that a three-parameter phase space fits the data as well. In its recent report, the ARGUS Collaboration [11] claims that the $\rho^0\rho^0$ threshold peak is dominated by the 2^+ partial wave. Clearly, this last result, if corroborated, does support the interpretation of the $\rho^0\rho^0$ peak as an exotic resonance. On the other hand, as has been properly pointed out by ARGUS, a small statistical or systematical error can alter the relative contributions of the 0^+ and 2^+ states. Furthermore, as stated in the ARGUS paper, their data could also be well fitted with an isotropic $\rho^0\rho^0$ hypothesis, as PLUTO was able to account for its $\rho^0\rho^0$ data in a phase-space fit.

The TCFM estimates for $\sigma(\gamma\gamma\to\phi\phi)$ and $\sigma(\gamma\gamma\to\rho^0\phi)$

are compatible with the experimental upper limits [4,7], which are quite higher. The additional set of input data needed for these calculations is the value for the $\gamma p \to \phi p$ cross section [20]. Since the photoproduction of ϕ is purely diffractive and the ϕ is a very narrow resonance, the above calculations are quite simple.

For the reaction $\gamma\gamma \to \omega\omega$, the TCFM estimates are much less reliable [10] because of two major deficiencies. First, it should be remembered that OPE, the predominant mechanism for this reaction, is not well estimated by t-channel factorization. In addition, we found it very difficult to isolate and assess the OPE contribution to $\sigma_{pp}^{\rm el}$. In fact, in an early attempt to estimate this input cross section [12], we assumed that $\sigma_{pp}^{\rm OPE} = \frac{1}{4}\sigma(np \to pn)$. This is not a very reliable assumption, as we know from the intermediate-energy study [21] of the np charge exchange, that the production mechanism of this reaction is quite complicated. If one, nevertheless, adopts this assumption, the TCFM output overestimates considerably the $\gamma\gamma \to \omega\omega$ cross section [7]. A more reliable estimate of the background of this channel clearly needs, above all, a better knowledge of the input data.

In contrast with the poor situation concerning the $\sigma_{pp}^{\rm OPE}$, we are quite able to separate the diffractive and OPE contributions to the $\gamma p \to \omega p$ reaction. This can be done [12] by either utilizing SU(3) relations between the $\gamma p \to V^0 p$ channels or by fitting the $\gamma p \to \omega p$ data [22] with an energy power expansion where the strong energy-dependent part is associated with OPE. The two methods yield compatible results. The availability of this input enables us to estimate the cross sections for the diffractive $\gamma \to \omega\phi$ and $\gamma\gamma \to \omega\rho^0$ channels. Our calculations are compatible with the experimental upper limits [7] for $\sigma(\gamma\gamma \to \omega\phi)$. As for the $\gamma\gamma \to \omega\rho^0$ channel, actual cross-section values as a function of energy have been reported [3,4,6,7]. The TPC/2γ and ARGUS Collaborations report a complex energy behavior structure which is not reproduced by the TCFM. These data are compared with our estimates in Fig. 3. In contrast, JADE reports a smooth cross section, which is well described by our predictions. We consider our calculations as a fair reproduction of a nonresonating background for this channel bearing in mind the following.

(1) We have estimated only the diffractive contribution to the process $\gamma\gamma \to \omega\rho^0$. There is also a OPE contribution

$$\sigma^{\rm OPE}(\gamma\gamma \to \omega\rho^0) = [\sigma^{\rm OPE}(\gamma\gamma \to \omega\omega)\sigma^{\rm OPE}(\gamma\gamma \to \rho^0\rho^0)]^{1/2} , \quad (10)$$

which presumably is rather small.

(2) The $\gamma\gamma \to \omega\rho^0$ data show a substructure at $W_{\gamma\gamma} < 1.4$ GeV. This has been attributed [7] to an $a_2(1320)$ formation in the direct $\gamma\gamma$ channel and should then be added to our "background" calculations.

(3) Some of the data show also a sizable peak at $W_{\gamma\gamma} \simeq 1.9$ GeV, which is not reproduced by the TCFM. This may be associated with a similar structure observed [7] in the $\gamma\gamma \to \omega\omega$ channel. Thus, in the framework of our model, this peak is not part of the background, which, according to our estimate, can account only for

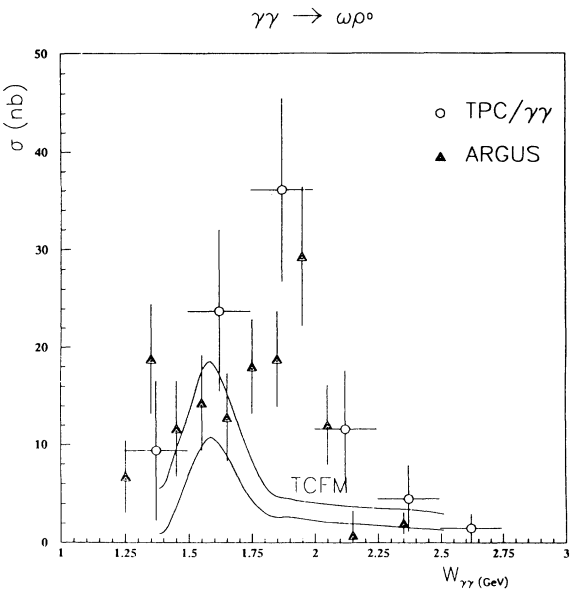

FIG. 3. Measured $\sigma(\gamma\gamma \to \omega\rho^0)$ compared with the TCFM expectation.

10–20% of the observed cross section in that mass range. However, as mentioned above, this peak has not been observed by JADE, which leaves the experimental situation ambiguous.

The TCFM analysis for the $\gamma\gamma \to \rho^+\rho^-$ and $\gamma\gamma \to K^{*+}K^{*-}$ is currently handicapped by the fact that we are unable to isolate in an unambiguous way the various t-channel exchanges from the input data. Notwithstanding this difficulty, we note that the TCFM estimates are compatible with these observed $\gamma\gamma$ cross sections. The relatively low $\sigma(\gamma\gamma \to \rho^+\rho^-)$ is associated with the small contribution of the isovector exchange to the photoproduction reaction $\gamma p \to \rho^+ n$. We also note that the shape of the observed enhancement [7] in $\gamma\gamma \to K^{*+}K^{*-}$ is compatible with the shape of the kinematical correction $F_{\gamma p}^2/(F_{\gamma\gamma}F_{p\Lambda(\Sigma)})$. However, since we are unable to support these speculations with an acceptable calculation, we can only safely conclude that the TCFM provides a reasonable background for the diffractive $\gamma\gamma \to V_1 V_2$ channels.

IV. $\gamma\gamma \to$ HADRON TOTAL CROSS SECTION

As we have noted in Sec. II, the high-energy factorization property of elastic amplitudes implies through the optical theorem that [23]

$$\sigma_{\gamma\gamma}^{\rm tot} = [\sigma_{\gamma p}^{\rm tot}]^2/\sigma_{pp}^{\rm tot} \simeq 300 \text{ nb} . \quad (11)$$

TCFM defines the continuation of Eq. (11) to low energies to be

$$\sigma_{\gamma\gamma}^{\rm tot} = \frac{[\sigma_{\gamma p}^{\rm tot}]^2}{\sigma_{pp}^{\rm tot}} \frac{F_{\gamma p}}{\sqrt{F_{\gamma\gamma}F_{pp}}} , \quad (12)$$

where all terms in Eq. (12) are evaluated for each t-channel contribution at the same incoming momentum p^*. We have thus

$$\frac{F_{\gamma p}}{\sqrt{F_{\gamma\gamma}F_{pp}}}=\frac{W_{\gamma p}}{\sqrt{W_{\gamma\gamma}W_{pp}}}\ , \tag{13}$$

where

$$W_{\gamma\gamma}=2p^*,\quad W_{\gamma p}=p^*+(p^{*2}+m_p^2)^{1/2}\ ,$$

and

$$W_{pp}=2(p^{*2}+m_p^2)^{1/2}\ .$$

For simplicity, we assume that each of the input γp and pp total cross sections can be parametrized as

$$\sigma_{ij}^{\rm tot}=A_{ij}+\frac{B_{ij}}{W_{ij}}\ , \tag{14}$$

where $W_{ij}=\sqrt{s_{ij}}$ is the c.m. total energy. The numerical input cross-section values given in this parametrization are [24,25]

$$\sigma_{\gamma p}^{\rm tot}=(98.0+88.9/W_{\gamma p})\ \mu{\rm b} \tag{15a}$$

and

$$\sigma_{pp}^{\rm tot}=(36.9+14.0/W_{pp})\ {\rm mb}\ , \tag{15b}$$

where the above parametrization is valid for $0.75<p^*<2.0$ GeV, corresponding to $1.5<W_{\gamma\gamma}<4$ GeV.

In order to calculate the output total cross section down to threshold, we have examined three options.

(1) Similar to our analysis of the $\gamma\gamma\to\rho^0\rho^0$ reaction, we assume that the low-energy γp and pp input channel are essentially diffractive with a threshold enhancement described by a $1/W$ factor for each of the reactions entering the TCFM relation. This means that Eq. (12) will read

$$\sigma_{\gamma\gamma}^{\rm tot}=\frac{(A_{\gamma p}W_{\gamma p}+B_{\gamma p})^2}{A_{pp}W_{pp}+B_{pp}}\left[\frac{W_{pp}}{W_{\gamma\gamma}W_{\gamma p}^2}\right]^{1/2}\ , \tag{16}$$

which will be referred to here as the ALM (Alexander-Levy-Maor) approach.

(2) Following Ref. [25], we assume that the relevant input cross section has a constant diffractive term plus an energy-dependent Regge-like component. In this case Eq. (12) reads

$$\sigma_{\gamma\gamma}^{\rm tot}=\frac{A_{\gamma p}^2}{A_{pp}}\left[\frac{W_{\gamma p}^2}{W_{pp}W_{\gamma\gamma}}\right]^{1/2}+\frac{B_{\gamma p}^2}{B_{pp}}\left[\frac{W_{pp}}{W_{\gamma\gamma}W_{\gamma p}^2}\right]^{1/2}\ , \tag{17}$$

to which we will refer here as the AMM (Alexander-Maor-Milstène) approach. A reasonable margin of error for both ALM and AMM approaches would be $\pm 15\%$.

(3) An alternative method to estimate $\sigma_{\gamma\gamma}^{\rm tot}$ was suggested by Levy [26]. In this approach one combines factorization with the optical theorem and uses measured Compton forward-scattering data and pp forward-elastic-scattering data to obtain

$$\sigma_{\gamma\gamma}^{\rm tot}=\frac{4\sqrt{\pi}[d\sigma(\gamma p\to\gamma p)/dt]_{t=0}}{\sqrt{[d\sigma(\gamma p\to\gamma p)/dt]_{t=0}}}\frac{F_{\gamma p}}{\sqrt{F_{pp}F_{\gamma\gamma}}}\ . \tag{18}$$

We refer to the resulting $\sigma_{\gamma\gamma}^{\rm tot}$ output from this relation as the Levy output.

Our output estimates together with the relevant data [27–29] are shown in Fig. 4. As can be seen, the three sets of output estimates differ in the low-energy domain with the ALM approach being the least divergent. A major difficulty in this analysis stems from our inability to determine the experimental behavior of $\sigma_{\gamma\gamma}^{\rm tot}$ at low energies. The cross sections reported by the PLUTO Collaboration [27] show a low-energy enhancement which is compatible with the TCFM. The TPC/2γ [28] and MD-1 [29] experiments (not shown) suggest that $\sigma_{\gamma\gamma}^{\rm tot}$ is almost flat at low energies. If systematic errors are taken into account, one may still consider the three experiments to be consistent among themselves, with the result that essentially no significant information does exist on the low-energy behavior of the $\gamma\gamma\to$ hadron cross section. Furthermore, it has recently been pointed out that the inclusive total $\gamma\gamma$ cross-section measurements, shown in Fig. 4, are currently lower in some low-$W_{\gamma\gamma}$ regions than the sum of the measured exclusive $\gamma\gamma$ hadron channels [30]. It is interesting to note that the low-energy enhancement of $\sigma_{\gamma\gamma}^{\rm tot}$ expected by the TCFM is consistent with a diffractive interpretation of the $\gamma\gamma\to\rho^0\rho^0$ enhancement. If that enhancement is a result of an exotic resonance formation, we do expect the forward $\gamma\gamma$ amplitude to have a large real component. In such a case the low-energy $\rho^0\rho^0$ enhancement would not imply a similar enhancement in the total $\gamma\gamma$ cross section. It is reasonable therefore to expect that an experimental clarification of the low-energy dependence of $\sigma_{\gamma\gamma}^{\rm tot}$ would help in understanding the mechanism responsible for the $\gamma\gamma\to\rho^0\rho^0$ enhancement.

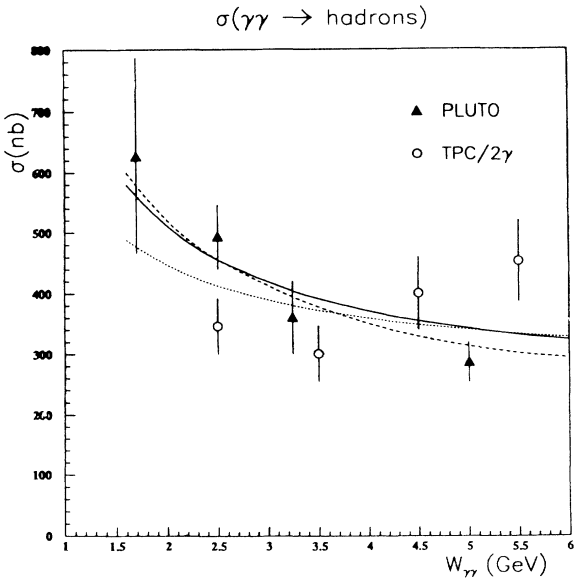

FIG. 4. Compilation of the total $\gamma\gamma\to$ hadrons cross section as a function of $W_{\gamma\gamma}$ from PLUTO [27] and TPC/2γ [28] experiments. The data are compared with the TCFM expectations: ALM (dots), AMM (solid line), and Levy (dashed line). Errors on the expectations due to input uncertainties are typically 10%.

V. SINGLE-TAG INTERACTIONS

It is interesting to examine the utilization of the TCFM for single-tag $\gamma^*\gamma$ interactions, i.e., the reaction between a virtual off-mass-shell probing photon ($M^2=-Q^2$) and a target quasireal photon. Data are available on single $\rho^0\rho^0$ production and on the total $\gamma^*\gamma\rightarrow$ hadron cross section, which is related to the photon structure function by

$$\sigma_{\gamma\gamma}^{\text{tot}}=\frac{4\pi\alpha^2}{Q^2}F_2^{\gamma}(x,Q^2)\ . \tag{19}$$

Our analysis relates directly to the unsolved problem of how to separate between the contributions of the pointlike and hadronlike components of the photon. In our treatment of the no-tag (i.e., two quasireal) $\gamma\gamma$ interactions, we have implicitly assumed that both the probing and target photons are essentially hadronlike and hence have considered their low-energy interactions as just another channel of hadron collisions. This vector-dominance-model- (VDM-) like assumption does not apply in the kinematic domain of deep-inelastic e-γ scattering, where $Q^2\gg 0$. As will be shown further on, the results of our analysis seem to suggest that the TCFM may be utilized to estimate the hadronlike component of the $\gamma^*\gamma$ reactions.

In order to estimate the single-tag production of $\rho^0\rho^0$, we use the low $Q^2<5$ GeV^2 data [31] of the $ep\rightarrow e\rho^0 p$ reaction. Our results are compared in Fig. 5 with the recent published data of PLUTO [32]. Compatible data on $\gamma\gamma\rightarrow 2\pi^+2\pi^-$ have also been reported by the TASSO Collaboration [33]. However, that analysis did not explicitly estimate the $\rho^0\rho^0$ signal in the 4π data. Two main features are seen in the data.

(1) The substantial $\rho^0\rho^0$ enhancement observed in the no-tag $Q^2=0$ data is sustained also at these low-Q^2 single-tag measurements.

(2) The Q^2 dependence of the integrated cross sections is well reproduced by a VDM Q^2 dependence. This is in contrast with the measured single-tag $\gamma^*\gamma$ cross sections, where it is well known that the VDM underestimates the data at $Q^2>1$ GeV^2.

These two observations are well reproduced by the TCFM. The success of the TCFM is not surprising if one recalls that it is expected that the low-Q^2 production of $\rho^0\rho^0$ is dominated by hadronlike photons.

The application of the TCFM to deep-inelastic e-γ scattering is similar to our treatment of $\sigma_{\gamma\gamma}^{\text{tot}}$, namely,

$$\sigma_{\gamma\gamma}(Q^2,W_{\gamma\gamma})=\frac{\sigma_{\gamma p}^2(Q^2,W_{\gamma p})}{\sigma_{pp}(W_{pp})}\frac{F_{\gamma p}}{\sqrt{F_{\gamma\gamma}F_{pp}}}\ , \tag{20}$$

where Eq. (20) is evaluated for each t-channel exchange at the same c.m. momentum p^*. We keep in mind that

$$F_2^{\gamma}(x_{\gamma},Q^2)=\frac{Q^2}{4\pi\alpha^2}\sigma_{\gamma\gamma}(Q^2,W_{\gamma\gamma})\ , \tag{21}$$

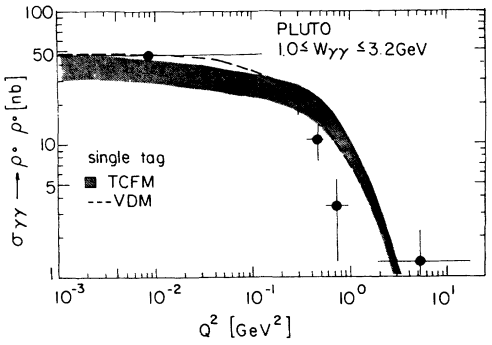

FIG. 5. Measured $\sigma(\gamma^*\gamma\rightarrow\rho^0\rho^0)$ as a function of Q^2 compared with the TCFM expectations.

$$F_2^{p}(x_p,Q^2)=\frac{\nu K}{4\pi\alpha^2}\frac{Q^2}{Q^2+\nu^2}\sigma_{\gamma p}(Q^2,W_{\gamma p})\ , \tag{22}$$

where

$$K=\frac{W_{\gamma p}^2-m_p^2}{2m_p},\quad \nu=K+\frac{Q^2}{2m_p}\ ,$$

and

$$W_{\gamma p}^2=2m_p\nu+m_p^2-Q^2\ .$$

The data input needed for the TCFM calculations is obtained from the deep-inelastic e-p scattering [34].

The Q^2 dependence of $F_2^{\gamma}(x_{\gamma},Q^2)$ and $\sigma_{\gamma\gamma}(Q^2,W_{\gamma\gamma})$ was examined some time ago [27]. It was shown that the TCFM provides an adequate reproduction of the data for $Q^2<5$ GeV^2. The model underestimates the higher-Q^2 data. This deficiency of the model is not surprising since the TCFM was constructed as a model for hadron interactions and its applicability to the photon pointlike sector is questionable at best. It is, however, quite reasonable to assume that the TCFM provides a realistic estimate for the hadron sector contribution to low-energy $\gamma^*\gamma$ collisions. If this indeed is the case, a simple parametrization of F_2^{γ} is suggested by Eqs. (20)–(22). This should be then supplemented by the noncoherent addition of the pointlike contribution to F_2^{γ}.

VI. CRITICAL ASSESSMENT

The main deficiency of our model is that the procedure we have just outlined, reasonable as it may be, is not unique. One may construct some other methods of extrapolation. To illustrate this point we consider two alternative models. For example, we may choose [19] to apply factorization to $d\sigma/d\Omega$ rather than to $d\sigma/dt$. In this way, when integrating, we eliminate the dependence of the integration limits on the energy and external masses. In such a method Eqs. (1) and (5) are replaced by

$$\frac{d\sigma}{d\Omega}=\frac{1}{4\pi s}\frac{\lambda(s,m_c^2,m_d^2)}{\lambda(s,m_a^2,m_b^2)}|f(s,t)|^2 \tag{23}$$

and

$$\sigma(a+b\to c+d)=\sum_i \frac{\sigma^i(a+y\to c+y)\sigma^i(x+b\to x+d)}{\sigma(x+y\to x+y)}\left[\frac{F_{ay}F_{xb}F_{cd}}{F_{cy}F_{xd}F_{ab}}\right]^{1/2}. \quad (24)$$

This is obviously a different and less singular extrapolation than ours. Its ability to produce a threshold $\gamma\gamma\to\rho\rho$ enhancement depends on the fine details of the $\sigma^2(\gamma p\to\rho p)/\sigma(pp\to pp)$ input at exceedingly small $p^*_{\rm out}$.

The suggested TCFM has three prominent features on which we wish to elaborate in some detail.

(1) The model depends on the input cross section and as such has no free parameters. This being the case, the reliability of the output depends essentially only on the quality and reliability of the input material. This is most crucial when we examine wide resonance production, such as $\gamma\gamma\to\rho^0\rho^0$, where a misinterpretation of the unfolded cross section $\tilde{\sigma}(\gamma p\to mp)$ may radically change the output. One must therefore examine the stability of the output against changes in the input.

(2) Factorization is not equally valid for different t-channel exchanges. In the high-energy limit we deal only with the elastic and diffractive channels for which factorization is well established [13]. At intermediate energies we also have to deal with the Regge trajectories, for which factorization is rather approximate at best, and the secondary π and K exchanges, for which factorization is badly broken because of strong absorptive effects (or Regge cuts). Intuitively, we expect, therefore, the TCFM to provide estimates that are more reliable for the diffractive $\gamma\gamma$ channels than for the nondiffractive ones. In particular, we are prone to suspect the reliability of estimates corresponding to π or K exchanges.

(3) The TCFM, by its construction, has a limited predictive power. Our main expectation is to obtain a reasonable average estimate of the low-energy diffractive $\gamma\gamma$ cross sections. We note, nevertheless, that our input assumptions imply that the low-energy diffractive background consists of a few partial waves at the least.

Clearly, the novelty of the TCFM is in its ability to generate a threshold enhancement in the cross section which is not a resonance state. In search for supporting evidence to this TCFM ability, it is instructive to examine the reaction $K^+p\to K^0\Delta^{++}$. This reaction has some properties which make it very attractive as a test case for the TCFM: namely, (1) the experimental integrated cross-section values [35] as a function of W_{Kp} have a resonancelike behavior close to threshold similar in shape to the one observed in $\sigma(\gamma\gamma\to\rho^0\rho^0)$; (2) the final state has the $\Delta^{++}(1232)$, which is a wide resonance; and (3) the reaction has been studied in the past extensively, and no evidence has been found for the existence of an exotic s-channel $S=+1$, $B=+1$ resonance.

In the intermediate-energy region this reaction is well reproduced by a ρ-a_2 exchange-degenerate Regge-pole model [36]. Thus, assuming that the ρ and a_2 are strongly exchange degenerate, we can derive from the TCFM the relation

$$\sigma(K^+p\to K^0\Delta^{++}) = \frac{\sigma(\pi^+p\to\pi^0\Delta^{++})\sigma(K^+n\to K^0p)}{\sigma(\pi^-p\to\pi^0n)}\frac{F_{\pi p}F_{Kn}}{F_{\pi p}F_{Kp}}, \quad (25)$$

for which reasonably good input data exist [35,37]. The Δ^{++} width is handled in accordance with Eqs. (6) and (7).

The results of the TCFM calculations together with the measured data values [18] are shown in Fig. 6. The calculated shaded band in the figure corresponds to the experimental errors of the input data. Considering the crudeness of our exchange-degeneracy assumption, which leaves the TCFM calculation parameter-free, we find that our ability to reproduce approximately the shape and normalization of the measured $\sigma(K^+p\to K^0\Delta^{++})$ near threshold, including the low-mass enhancement, is rather remarkable. We further note that this result also strongly supports our choice of $p^*_{\rm out}$ as the appropriate variable for the low-energy phase-space correction. The above example is, however, insensitive to flux corrections, as the ratio of the fluxes given in Eq. (25) is approximately equal to unity.

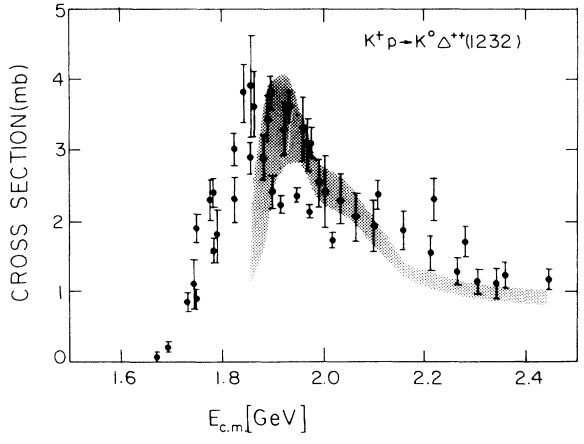

FIG. 6. Expectation of the TCFM (shaded area) for the reaction $\sigma(K^+p\to K^0\Delta^{++}(1232))$ as a function of $E_{\rm c.m.}$ compared with measured values (data points) given in Ref. [35].

VII. CONCLUSIONS

The main conclusion of our investigation is that the TCFM provides a reasonable estimate of low-energy diffractive integrated cross sections. Our examination of the reaction $K^+p\to K^0\Delta^{++}(1232)$ suggests that the model is applicable also for the low-energy continuation of reactions dominated by Regge exchanges in the intermediate-energy range.

The main use of the TCFM has been in the analysis of diffractive $\gamma\gamma$ reactions, where we are able to reproduce the diffractive $\gamma\gamma\to V_1V_2$ channels for no-tag and single-tag data. Thus we suggest, in the framework of our model, that the threshold enhancement observed in

$\gamma\gamma \to \rho^0\rho^0$ is a rather conventional hadronic phenomenon. This conventional interpretation serves also as a reminder that the mere observation of a cross-section threshold enhancement is not sufficient to establish the existence of a resonance, be it exotic or not. Hence we expect that the exotic signals, which were advocated as an explanation for this enhancement, even if they do exist, are small and superimposed on a larger background. An obvious check on our approach is obtained from the low-energy partial-wave analysis of the $\gamma\gamma \to \rho^0\rho^0$ channel, which presently is still experimentally unclear. An additional indirect check of our model can be obtained from the low-energy behavior of the total $\gamma\gamma \to$ hadron cross section, where we expect a threshold enhancement. Unfortunately, also in this case, the various experimental observations do not provide, as yet, a consistent picture.

ACKNOWLEDGMENTS

We with to thank A. Levy for his many contributions in the early stages of this work and for many helpful remarks. One of us (U.M.) wishes to thank the MINERVA Foundation and the U.S. Department of Energy, Contract No. DEAC02-76ER01195, for financial support.

[1] TASSO Collaboration, R. Brandelik *et al.*, Phys. Lett. **97B**, 448 (1980); M. Althof *et al.*, Z. Phys. C **16**, 13 (1982).

[2] Mark II Collaboration, D. L. Burke *et al.*, Phys. Lett. **103B**, 153 (1981).

[3] CELLO Collaboration, H. J. Behrend *et al.*, Z. Phys. C **21**, 205 (1984); Phys. Lett. B **218**, 493 (1989); M. Feindt, in *Photon-Photon Collisions,* Proceedings of the VIII International Workshop, Shoresh, Jerusalem Hills, Israel, 1988, edited by U. Karshon (World Scientific, Singapore, 1988), p. 3.

[4] TPC/2γ Collaboration, H. Aihara *et al.*, Phys. Rev. D **37**, 28 (1988); M. Ronan, in *Photon-Photon Collisions* [3], p. 30.

[5] PLUTO Collaboration, Ch. Berger *et al.*, Z. Phys. C **38**, 521 (1988).

[6] JADE Collaboration, H. Kolanoski *et al.*, in *Photon-Photon Collisions,* Proceedings of the Fifth International Workshop, Aachen, West Germany, 1983, edited by Ch. Berger, Lecture Notes in Physics Vol. 191 (Springer, New York, 1983), p. 175; A. Wegener *et al.*, DESY Report No. 90-069 (unpublished).

[7] ARGUS Collaboration, H. Albrecht *et al.*, Phys. Lett. B **196**, 101 (1987); **198**, 255 (1988); **217**, 205 (1989).

[8] N. N. Achasov, S. A. Deryanin, and G. N. Shestakov, Phys. Lett. **108B**, 134 (1982); Z. Phys. C **16**, 55 (1982); **27**, 99 (1985).

[9] B. A. Li and K. F. Liu, Phys. Lett. **118B**, 435 (1982); **124B**, 550 (1982); Phys. Rev. Lett. **51**, 1510 (1983); Phys. Rev. D **30**, 613 (1984).

[10] U. Maor, in *Photon-Photon Collisions* [3], p. 282; A. Levy, in *Proceedings of the XXIV International Conference on High Energy Physics,* Munich, West Germany, 1988, edited by R. Kotthaus and J. H. Kühn (Springer, Berlin, 1988), p. 655.

[11] ARGUS Collaboration, H. Albrecht *et al.*, DESY Report No. 90-34 (unpublished); Phys. Lett. B **267**, 535 (1991).

[12] G. Alexander, U. Maor, and P. G. Williams, Phys. Rev. D **26**, 1198 (1982); G. Alexander, A. Levy, and U. Maor, Z. Phys. C **30**, 65 (1986).

[13] M. Gell-Mann, Phys. Rev. **8**, 263 (1962); V. N. Gribov and I. Ya. Pomeranchuk, Phys. Rev. Lett. **8**, 343 (1962); **8**, 412 (1962).

[14] J. D. Jackson, Nuovo Cimento **34**, 1644 (1964).

[15] CEA Collaboration, H. R. Crouch *et al.*, Phys. Rev. **146**, 994 (1966).

[16] ABBHHM Collaboration, R. Erbe *et al.*, Phys. Rev. **175**, 1669 (1968).

[17] O. Benary, L. P. Price, and G. Alexander, Report No. UCRL-20000, 1970 (unpublished).

[18] F. Arash, M. J. Moravcsik, and G. Goldstein, Phys. Rev. D **32**, 74 (1985); see also, e.g., a summary by A. Bohr and B. R. Mottelson, *Nuclear Structure* (Benjamin, New York, 1969), p. 264.

[19] H. Kolanoski, Z. Phys. C **39**, 534 (1988).

[20] D. G. Cassel *et al.*, Phys. Rev. D **24**, 2787 (1981).

[21] E. Gotsman and U. Maor, Nucl. Phys. **B145**, 459 (1978).

[22] Y. Eisenberg *et al.*, Phys. Lett. **34B**, 439 (1971); J. Ballam *et al.*, Phys. Rev. D **7**, 3150 (1973); see also Ref. [20].

[23] The application of factorization to the $\gamma\gamma$ total cross section in its high-energy approximation was previously given by S. J. Brodsky *et al.*, Phys. Rev. D **4**, 1532 (1971); J. L. Rosner, BNL Report No. 17552, 1972 (unpublished), p. 316, and by V. M. Budnev *et al.*, Phys. Rep. C **15**, 181 (1975).

[24] G. Wolf, in *Proceedings of the 1971 International Symposium on Electron and Photon Interactions at High Energies,* edited by N. B. Mistry (Cornell University Press, Ithaca, 1971), p. 189.

[25] G. Alexander, U. Maor, and C. Milsténe, Phys. Lett. **131B**, 224 (1983).

[26] A. Levy, Phys. Lett. B **177**, 106 (1986); **181**, 401 (1986).

[27] PLUTO Collaboration, Ch. Berger *et al.*, Phys. Lett. **149B**, 421 (1984).

[28] TPC/2γ Collaboration, D. Bintinger *et al.*, Phys. Rev. Lett. **54**, 763 (1985); H. Aihara *et al.*, report (unpublished).

[29] MD-1 Collaboration, A. E. Blinov *et al.*, Novosibirsk Report No. 85-95 (unpublished), and the updated version, S. E. Baru *et al.*, in *Proceedings of the XXIII International Conference on High Energy Physics,* Berkeley, California, 1986, edited by S. Loken (World Scientific, Singapore, 1987).

[30] G. Alexander and G. Bella (private communication).

[31] I. Cohen *et al.*, Phys. Rev. D **25**, 634 (1982).

[32] PLUTO Collaboration, Ch. Berger *et al.*, Z. Phys. C **38**, 521 (1988).

[33] TASSO Collaboration, W. Braunschweig *et al.*, Z. Phys. C **41**, 353 (1988).

[34] B. A. Gordon *et al.*, Phys. Rev. D **20**, 2645 (1979).

[35] See, e.g., V. Flamino *et al.*, *Compilation of Cross Sections II: K^+ and K^- Induced Reactions* (Report No. CERN-HERA 83-01, 1983).

[36] M. Kramer and U. Maor, Nucl. Phys. **B13**, 651 (1969).

[37] See, e.g., V. Flamino *et al.*, *Compilation of Cross Sections I: π^+* and *π^- Induced Reactions* (Report No. CERN-HERA 83-01, 1983).

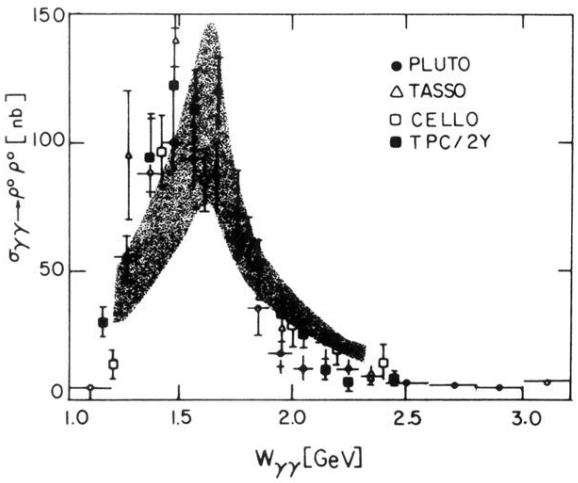

FIG. 1. Data compilation of $\sigma(\gamma\gamma\to\rho^0\rho^0)$ as a function of $W_{\gamma\gamma}$ compared with the expectation of the TCFM (shaded band).

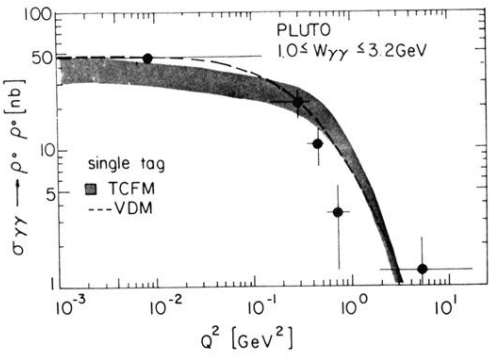

FIG. 5. Measured $\sigma(\gamma^*\gamma \to \rho^0\rho^0)$ as a function of Q^2 compared with the TCFM expectations.

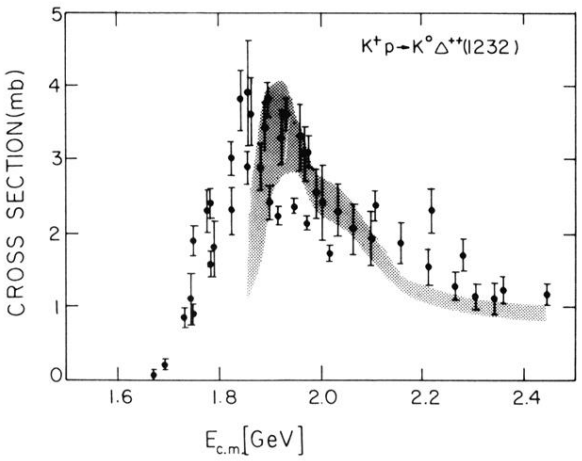

FIG. 6. Expectation of the TCFM (shaded area) for the reaction $\sigma(K^+p \to K^0\Delta^{++}(1232))$ as a function of $E_{c.m.}$ compared with measured values (data points) given in Ref. [35].